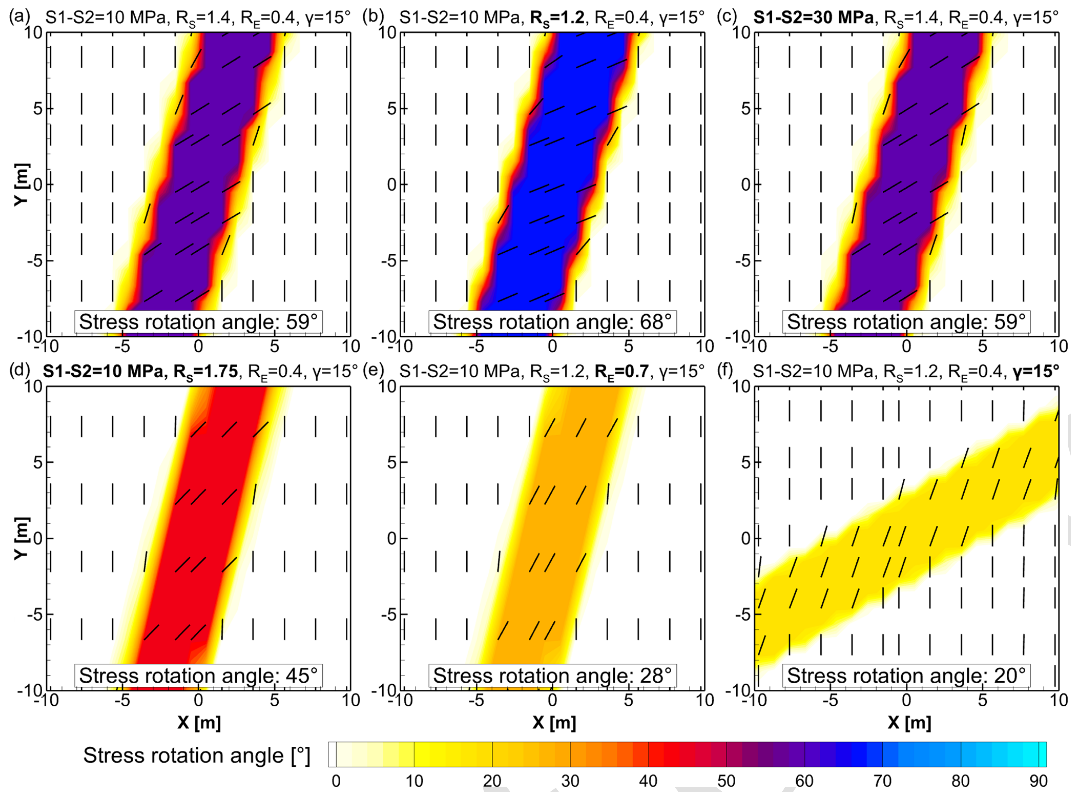

Figure 3. Influence of different parameters on the stress rotation angle. The stress rotation is colour coded and shown as vectors or lines that indicate the S_1 orientation due to a material contrast in the fault core area (Fig. 2c). **(a)** A basic setting with a fault that is 15° deviated from the orientation of S_1, a differential stress of 10 MPa, a stress ratio of $R_S = 1.4$, and a rock stiffness contrast of $R_E = 0.4$ ($E = 16$ GPa in the fault core and $E = 40$ GPa in the host rock. This reference setting is compared with stress rotation based on individually changed parameters (bold in titles of **b**– **f**). **(b)** $R_S = 1.2$. **(c)** Differential stress increased to 30 MPa and $R_S = 1.2$. **(d)** Differential stress increased to 30 MPa with the same S_2 magnitude as in **(a)**, $R_S = 1.75$. **(e)** $R_E = 0.7$. **(f)** Deviation of 45° between fault strike and the S_1 orientation. All parameters of all panels are comprehensively listed in Table 2.

A decrease in the stress ratio to $R_S = 1.2$ while the differential stress S_1–S_2 remains constant (but the magnitudes of the principal stresses change to $S_1 = 60$ MPa and $S_2 = 50$ MPa) leads to an increased stress rotation angle of 68° (Fig. 3b). An increase in S_1–S_2 from 10 to 30 MPa ($S_1 = 105$ MPa, $S_2 = 75$ MPa) while $R_S = 1.4$ and therefore constant results in the same rotation angle of 59° as in the reference case (Fig. 3c). In contrast, an increase in S_1–S_2 to 30 MPa ($S_1 = 70$ MPa, $S_2 = 40$ MPa) with a change in stress ratio to $R_S = 1.75$ results in a decrease in stress rotation to 45° (Fig. 3d). This indicates that it is rather the stress ratio R_S that controls the stress rotation than the differential stress S_1–S_2. A more comprehensive comparison is shown in Table 3, which indicates the independence of stress rotation angle from differential stress S_1–S_2 and its dependence on stress ratio R_S.

A reduction in the stiffness contrast from $R_E = 0.4$ to $R_E = 0.7$ means that the fault is stiffer and thus closer to the host rock's stiffness. This results in a reduction in the stress rotation of 31 to 28° (Fig. 3e). This positive correlation of rock stiffness contrast R_E to potential stress rotation angle has been observed previously (Reiter, 2021). It is intuitive in that with the assumptions made herein the same stiffness in fault and host rock ($R_E = 1$) cannot lead to any rotation at all. Thus, greater stiffness contrast (small values for R_E) promote less stress rotation.

An increase in the angle γ between the fault strike and the far-field S_1 orientation from initially 15° to now 45° results in a smaller rotation angle of 19° (Fig. 3f). The angle γ is thus negatively correlated with the rotation angle. No rotation is expected for faults that strike perpendicular to the S_1 orientation ($\gamma = 90°$). Large stress rotation angles are expected for faults that strike with a low angle towards the S_1 orientation.

3.2 Spatial effects

As already indicated in Fig. 3, stress rotation is observed only directly in the fault zone where a rock stiffness contrast R_E exists. In order to investigate its influence beyond the fault itself we display the stress rotation angle as a function of distance normal to the fault (Fig. 4). In this idealized representation of a fault without a damage zone, no signifi-

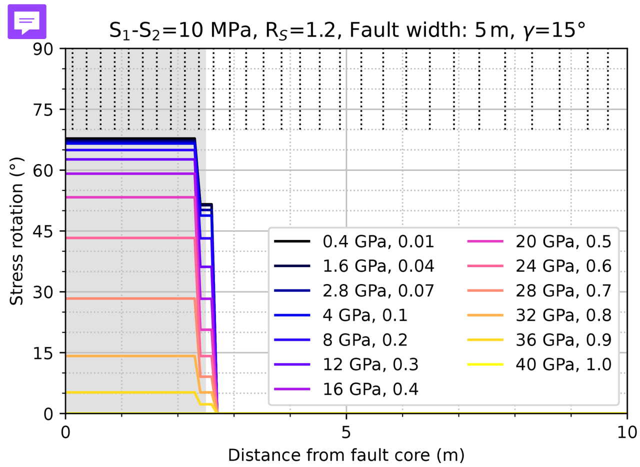

Figure 4. Intrinsic stress rotation in the fault zone as a function of increasing rock stiffness contrast. The abrupt change from a rotated to a far-field stress state is observed at the border of the fault. The rotation is shown perpendicular to the fault. The rock stiffness contrast between the fault's Young's modulus and a host rock stiffness of $E_{\mathrm{host}} = 40\,\mathrm{GPa}$ is colour coded and indicated in the legend as absolute values in GPa and ratio R_{E}. For reference, the purple line $R_{\mathrm{E}} = 0.4$ is taken from Fig. 3a, while the orange line $R_{\mathrm{E}} = 0.7$ is taken from Fig. 3e. See also Table 2. The distance from the fault core centre (x axis) in relation to the stress rotation (y axis) is shown. The vertical dotted lines at the top indicate the discretization normal to the fault strike with an element size of 25 cm within the fault and increasing outside the fault. Please note that the distance is from the fault core centre, and thus only half of the fault width is shown here in grey.

an individual diagram (panels of Fig. 5). Within each diagram, the angle γ between fault strike and S_1 orientation is related to the modelled stress rotation angle. Each model scenario with an individual set of parameters is now displayed as a point in a diagram (Fig. 5). The material contrast R_{E} is colour coded. Four different stress ratios R_{S} are compared in the four panels of Fig. 5.

The initial observation is the importance of the angle γ. Structures with a significant contrast in rock stiffness that are perpendicular to the far-field orientation of S_1 ($\gamma = 90°$) do not exhibit any rotation of the principal stress axes at all. This is independent of all other parameters. In turn, structures parallel to the S_1 orientation ($\gamma = 0°$) can rotate by up to 90°. This signifies a mutual replacement of S_1 and S_2 orientation. Whether a stress rotation of 90° is reached or not is tied to the ratios R_{E} and R_{S}.

For large contrasts (i.e. small R_{E}) and small R_{S} values, the maximum stress rotation angle is reached in several scenarios. At the same time, high R_{E} values limit the maximally achieved stress rotation angle. The maximum angle for any given R_{E} value is then up to 90° and controlled by the stress ratio R_{S} (Fig. 5). However, in these cases the maximum angle is not observed for $\gamma = 0°$ but for angles $0° < \gamma < 45°$. Apparently, for an angle $\gamma = 0°$ either no stress rotation at all or the maximally possible stress rotation of 90° occurs.

The large influence of the R_{S} value is additionally displayed in a representation of the three model parameters investigated in this study, where the decisiveness of the R_{S} value becomes apparent (Fig. 6). This is particularly observable for $R_{\mathrm{E}} = 0.6$ at faults that are striking parallel to the S_1 orientation ($\gamma = 0°$). A low R_{S} of around 1.1 leads to a stress rotation of 90° (Fig. 5a). However, an increase in R_{S} to ≥ 1.5 (Fig. 6) prevents any stress rotation at all.

These results show that the previously indicated correlations (Fig. 3) can be confirmed. These correlations are as follows.

- A negative correlation between R_{S} and the stress rotation angle, i.e. large stress rotations for principal stress magnitudes that are similar to each other.

- A negative correlation between R_{E} and the stress rotation angle, i.e. large stress rotations for large material contrast (small values of R_{E}).

- A mostly negative correlation between the angle γ between strike angle vs. far-field S_1 orientation and the stress rotation angle, meaning that S_1 that acts normal to a faults strike will see no rotation. An exception is an angle of $\gamma = 0°$, where either no stress rotation or a rotation of 90° is observed.

This shows the combined influence of the stress ratio, the magnitude of material contrast, and the orientation of the fault strike compared to the far-field stress state on the angle of stress rotation. The expected angle of stress rotation can be estimated if all corresponding data are available.

In addition to the previously mentioned correlations, further rules can be observed in Fig. 5. The sum of the angle between fault strike and far-field stress orientation γ and the angle of observed stress rotation cannot exceed 90°. No rotation is observed if the fault strikes perpendicular to the far-field stress orientation, i.e. $\gamma = 90°$. A rotation of 90° is only possible if $\gamma = 0°$. However, a rotation of 90° is not observed for all scenarios with $\gamma = 0°$. Whether any rotation is observed or not depends on the stiffness contrast. This highlights the importance of all three parameters on the expected angle of stress rotation.

4 Discussion

The influence of the rock stiffness contrast R_{E}, the stress ratio R_{S}, and angle between a fault or a geological structure and the far-field S_1 orientation on the rotation of the principal stress axes are derived from a generic study using a 2D plane strain numerical model. The results indicate the importance of the aforementioned parameters on the possibility of occurrence and expected angle of stress rotation. They are

Proof only